Monthly Notices
of the
ROYAL ASTRONOMICAL SOCIETY

MNRASL **433,** L1–L5 (2013)
Advance Access publication 2013 May 22

doi:10.1093/mnrasl/slt034

Systematic investigation of the expected gravitational wave signal from supermassive black hole binaries in the pulsar timing band

A. Sesana⋆

Max-Planck-Institut für Gravitationsphysik, Albert Einstein Institut, Am Muhlenberg 1, D-14476 Golm, Germany

Accepted 2013 March 11. Received 2013 March 8; in original form 2012 November 22

ABSTRACT

In this Letter, we carry out the first systematic investigation of the expected gravitational wave (GW) background generated by supermassive black hole (SMBH) binaries in the nHz frequency band accessible to pulsar timing arrays (PTAs). We take from the literature several estimates of the redshift-dependent galaxy mass function and of the fraction of close galaxy pairs to derive a wide range of galaxy merger rates. We then exploit empirical black hole–host relations to populate merging galaxies with SMBHs. The result of our procedure is a collection of a large number of phenomenological SMBH binary merger rates consistent with current observational constraints on the galaxy assembly at $z < 1.5$. For each merger rate we compute the associated GW signal, eventually producing a large set of estimates of the nHz GW background that we use to infer confidence intervals of its expected amplitude. When considering the most recent SMBH–host relations, accounting for overmassive black holes in brightest cluster galaxies, we find that the nominal 1σ interval of the expected GW signal is only a factor of 3–10 below current PTA limits, implying a non-negligible chance of detection in the next few years.

Key words: black hole physics – gravitational waves – pulsars: general – galaxies: evolution.

1 INTRODUCTION

Precision timing of an array of millisecond pulsars (PTA) provides a unique opportunity to get the very first low-frequency gravitational wave (GW) detection. The European Pulsar Timing Array (EPTA; Ferdman et al. 2010), the Parkes Pulsar Timing Array (Manchester et al. 2013) and the North American Nanohertz Observatory for Gravitational Waves (Jenet et al. 2009), joining together in the International Pulsar Timing Array (IPTA; Hobbs et al. 2010) are constantly improving their sensitivity in the frequency range of $\sim 10^{-9}$–10^{-6} Hz. Inspiralling supermassive black hole (SMBH) binaries populating merging galaxies throughout the Universe are expected to generate the dominant signal in this frequency band (see e.g. Wyithe & Loeb 2003; Sesana, Vecchio & Colacino 2008). Theoretical models of SMBH evolution within the standard hierarchical framework of galaxy formation indicate a typical GW strain amplitude $A \sim 10^{-15}$ at a frequency $f = 1\ \mathrm{yr}^{-1}$ (Wyithe & Loeb 2003; Sesana et al. 2008; Ravi et al. 2012), with an uncertainty of $\approx$0.5 dex (Sesana et al. 2008). However, a recent investigation by McWilliams, Ostriker & Pretorius (2012), based on a phenomenological model in which the low-redshift massive galaxy assembly is driven by mergers only, predicts a higher background with a fiducial amplitude $A \sim 4 \times 10^{-15}$. Though useful, all the aforementioned models employ specific recipes for the galaxy assembly and/or for the growth of SMBHs, and a systematic investigation of the possible range of signals compatible with observational uncertainties is still missing. This is a particularly important issue to assess at this point for two reasons: (i) the best limit placed by PTAs on the GW background amplitude is $A = 6 \times 10^{-15}$ (van Haasteren et al. 2011), close to theoretical predictions; (ii) SMBHs in brightest cluster galaxies (BCGs) were recently inferred to be more massive than expected (Hlavacek-Larrondo et al. 2012),[1] resulting in a revision to the established SMBH–host relations (McConnell & Ma 2013; Scott, Graham & Schombert 2013) that might push the expected GW background level closer to current upper limits, implying possible detection in the next few years.

As part of the common effort of the EPTA collaboration to detect GWs with pulsar timing (van Haasteren et al. 2011), we present here the first *systematic investigation* of the range of GW signal amplitudes consistent with *observationally based* estimates of the SMBH assembly in the low-redshift Universe. This Letter is organized as follows. In Section 2, we describe our model for generating the GW background and we test it against a range of observational constrains; results are presented and discussed in Section 3. Throughout this Letter, we assume a concordance Λ cold dark matter universe with $\Omega_{\rm M} = 0.27$, $\Omega_{\lambda} = 0.73$ and $h = 0.7$. Unless otherwise specified, we use geometric units where $G = c = 1$.

⋆ E-mail: alberto.sesana@aei.mpg.de

[1] And even more puzzling is the case of NGC 1277 (van den Bosch et al. 2012).

2 BUILDING THE GW BACKGROUND FROM ASTROPHYSICAL OBSERVABLES

2.1 Mathematical description of the GW background

Consider a cosmological population of merging SMBH binaries. Each merging pair is characterized by the masses of the two holes $M_{\bullet,1} > M_{\bullet,2}$, defining the mass ratio $q_\bullet = M_{\bullet,2}/M_{\bullet,1}$.[2] Following Sesana et al. (2008) (see also Phinney 2001), the characteristic amplitude h_c of the GW signal generated by such population is given by

$$h_c^2(f) = \frac{4}{\pi f^2}\int\int\int \mathrm{d}z\,\mathrm{d}M_{\bullet,1}\mathrm{d}q_\bullet \frac{\mathrm{d}^3 n}{\mathrm{d}z\,\mathrm{d}M_{\bullet,1}\mathrm{d}q_\bullet}\frac{1}{1+z}\frac{\mathrm{d}E_{\rm gw}(\mathcal{M})}{\mathrm{d}\ln f_r}. \quad (1)$$

Here, the factor $(1+z)^{-1}$ accounts for the redshift of gravitons, and the energy emitted per logarithmic frequency interval is

$$\frac{\mathrm{d}E_{\rm gw}}{\mathrm{d}\ln f_r} = \frac{\pi^{2/3}}{3}\mathcal{M}^{5/3} f_r^{2/3}, \quad (2)$$

where we assumed circular binaries driven by GW emission only. $\mathcal{M} = (M_{\bullet,1}M_{\bullet,2})^{3/5}/(M_{\bullet,1}+M_{\bullet,2})^{1/5}$ is the chirp mass of the binary and $f_r = (1+z)f =$ is the GW rest-frame frequency, which is twice the binary Keplerian frequency. The quantity $\mathrm{d}^3 n/(\mathrm{d}z\,\mathrm{d}M_{\bullet,1}\mathrm{d}q_\bullet)$ represents the differential merger rate density (i.e. number of mergers per comoving volume) of SMBH binaries per unit redshift, mass and mass ratio. For convenience, we decided to keep it a function of $M_{\bullet,1}$ and $q_\bullet$ instead of $\mathcal{M}$ only.

It is straightforward to show (Phinney 2001) that the predicted characteristic amplitude scales as $\propto f^{-2/3}$, with a normalization that depends on the details of the merging binary population, and it is usually represented as (see e.g. Jenet et al. 2006)

$$h_c(f) = A\left(\frac{f}{\mathrm{yr}^{-1}}\right)^{-2/3}, \quad (3)$$

where A is a model-dependent constant that represents the amplitude of the signal at the reference frequency $f = 1\,\mathrm{yr}^{-1}$. Since observational limits on the GW background are usually given in terms of A (Jenet et al. 2006; van Haasteren et al. 2011; Demorest et al. 2013), we keep the parametrization given by equation (3) in this Letter, and we investigate the range of A predicted by phenomenological models of the SMBH assembly based on observations. It is worth mentioning that the shortcomings of equation (1) in catching the relevant features of the GW signal emitted by a realistic population of *quasi-monochromatic sources* were extensively investigated by Sesana et al. (2008), Sesana, Vecchio & Volonteri (2009) and Ravi et al. (2012). Although equation (1) fails in describing small number statistics effects and the intrinsic non-Gaussianity of the signal, it is sufficient to describe its expected overall amplitude, which is our main interest here.

2.2 Determination of the SMBH binary merger rate

Since the energy emitted per logarithmic frequency interval is fixed by General Relativity (in the approximation of circular GW-driven binaries), the typical background strength A depends on the SMBH binary differential merger rate only. In contrast to our past work (Sesana et al. 2008, 2009), we take here an observational approach to determine $\mathrm{d}^3 n/\mathrm{d}z\,\mathrm{d}M_{\bullet,1}\mathrm{d}q_\bullet$. We proceed in two steps: (i) we determine *from observations* the *galaxy* merger rate $\mathrm{d}^3 n_G/\mathrm{d}z\,\mathrm{d}M\,\mathrm{d}q$ (in a merging galaxy pair, M and $q < 1$ are the mass of the primary galaxy and the mass ratio, respectively), and (ii) we populate merging galaxies with SMBHs according to empirical black hole mass–galaxy host relations found in the literature.

2.2.1 Galaxy merger rate

The galaxy differential merger rate can be written as

$$\frac{\mathrm{d}^3 n_G}{\mathrm{d}z\,\mathrm{d}M\mathrm{d}q} = \frac{\phi(M,z)}{M\ln 10}\frac{\mathcal{F}(z,M,q)}{\tau(z,M,q)}\frac{\mathrm{d}t_r}{\mathrm{d}z}. \quad (4)$$

Here, $\phi(M,z) = (\mathrm{d}n/\mathrm{d}\log M)_z$ is the galaxy mass function measured at redshift z; $\mathcal{F}(M,q,z) = (\mathrm{d}f/\mathrm{d}q)_{M,z}$ is the differential fraction of galaxies with mass M at redshift z paired with a secondary galaxy having a mass ratio in the range $q, q+\delta q$; $\tau(z,M,q)$ is the typical merger time-scale for a galaxy pair with a given M and q at a given z and $\mathrm{d}t_r/\mathrm{d}z$ converts a proper time rate into a redshift rate and is given by standard cosmology. The reason for writing equation (4) is that ϕ and $\mathcal{F}$ can be directly measured from observations, whereas τ can be inferred by detailed numerical simulations of galaxy mergers, as discussed below.

We take three different galaxy stellar mass functions from the literature (Borch et al. 2006; Drory et al. 2009; Ilbert et al. 2010) and match them with the local mass function (Bell et al. 2003) to obtain three fiducial $\phi_z(M)$. To each fiducial mass function we add an upper and a lower limit accounting for the errors given by the authors on the function best-fitting parameters, plus an additional 0.1 dex systematic error due to uncertainties in the determination of the galaxy masses, for a total of nine galaxy mass functions. For all mass functions, we separate early-type and late-type galaxies. Total stellar masses are converted in bulge stellar masses by assuming appropriate bulge-to-total stellar ratios accounting for galaxy morphology as detailed in Section 2.2.2. We restrict our calculation to $z < 1.3$ and $M > 10^{10}\,\mathrm{M}_\odot$, since these are the systems contributing the largest fraction of the GW signal. By extrapolating our calculations, we found that merging pairs residing in galaxies with $M < 10^{10}\,\mathrm{M}_\odot$ or at $z > 1.3$ can contribute at most 5 per cent to the signal amplitude, and can be safely neglected.

We consider four studies of the evolution of the galaxy pair fraction (Bundy et al. 2009; de Ravel et al. 2009; López-Sanjuan et al. 2012; Xu et al. 2012). Pair identification techniques are very diverse, and more details about the advantages and shortcomings of each procedure will be discussed in our following paper (Sesana, in preparation). For our current scope, it is sufficient to note that every procedure returns pair fractions of order of few per cent, and most estimates are consistent within a factor of 2. Pair fractions are usually integrated over some range of q and are given in different mass bins in the form $f(z) = f_0(1+z)^\gamma$. A good proxy for the observed pair q distribution is $\mathrm{d}f/\mathrm{d}q \propto q^{-1}$. Given $f(z)$, we can therefore simply write $\mathrm{d}f/\mathrm{d}q(z) = -f(z)/(q\ln q_\mathrm{m})$, where q_m is the minimum mass ratio selected in counting pairs. Each author applies different criteria as for q_m, mass and redshift range, and the maximum projected distance d_max below which two galaxies are considered a bound pair, as detailed in Table 1. Also in this case, for each of the four fiducial models, we consider an upper and a lower limit taking into account the errors in the best-fitting parameters f_0, γ, as reported by the authors, to get a total of 12 pair fraction models. When necessary, we extrapolate the pair fraction estimates to cover the full mass and redshift range of interest ($z < 1.3$ and $M > 10^{10}\,\mathrm{M}_\odot$). When pair counting for different galaxy types are available, we apply them to the corresponding galaxy-type

[2] To avoid confusion, we denote the masses and mass ratio of the SMBH binary as $M_{\bullet,1}$, $M_{\bullet,2}$, $q_\bullet$, whereas plain M and q are used for galaxies.

Table 1. Overview of the pair fraction selection performed in the papers used in this work. See the text for details.

Paper	q_m	M_{min} ($M_\odot$)	d_{max} (kpc)	Gal. type
Bundy et al. (2009)	0.25	10^{10}	20	Yes
de Ravel et al. (2009)	0.25	$10^{9.5}$	100	No
Lopez et al. (2012)	0.25	10^{11}	30	Yes
Xu et al. (2012)	0.4	$10^{9.4}$	20	No

mass function, otherwise, we assume the same pair fraction for early- and late-type galaxies. López-Sanjuan et al. (2012) also provide pair fractions for 'minor mergers', i.e. for $0.25 > q > 0.1$. We checked that including those in our calculation enhances the background by a factor 0.06 dex ($\lesssim$15 per cent) at most.

Galaxy merger time-scales τ were carefully estimated by Kitzbichler & White (2008) using mock catalogues of galaxy pairs in the Millennium simulation (Springel et al. 2005). In their equation 10, they provide the average merger time-scale as a function of M, z and projected distance d_p. We complement their equation 10 with an $\approx q^{-0.3}$ dependence extracted by fitting the results of a set of full hydrodynamical simulation of galaxy mergers presented by Lotz et al. (2010). In doing this, we noticed that the merger time-scales given by Lotz et al. (2010) are a factor of 2 shorter than those given by Kitzbichler & White (2008); we therefore adopted two different normalizations to get a 'fast' and a 'slow' merger scenario.

We interpolate all the measured ϕ, $\mathcal{F}$, τ on a fine 3D grid in (z, M, q), to numerically obtain $9 \times 12 \times 2 = 216$ differential galaxy merger rates. Note that typical values of τ are of the order of a Gyr; therefore, the merger rate at a given (z, M, q) point in the grid is obtained by evaluating ϕ and $\mathcal{F}$ at ($z + \delta z$, M, q), where δz is the redshift delay corresponding to the merging time τ. Note that by doing this, we implicitly assume that all SMBH binaries coalesce instantaneously at the merger time of their hosts.

2.2.2 *Black hole–host relations*

We assign to each merging galaxy pair SMBHs with masses drawn from 11 different SMBH–galaxy relations found in the literature (see Table 2). We write them in the form

$$\log_{10} M_\bullet = \alpha + \beta \log_{10} X, \tag{5}$$

where $X = \{\sigma/200 \text{ km s}^{-1}, L_i/10^{11} L_{i,\odot} \text{ or } M_{bulge}/10^{11} M_\odot\}$, being σ the stellar velocity dispersion of the galaxy bulge, L_i its mid-infrared luminosity and M_{bulge} its stellar mass. Each relation is characterized by an intrinsic scatter ϵ. α, β, ϵ are listed in Table 2. The relations link $M_\bullet$ to the *bulge* properties, whereas our galaxy merger rates are function of the total stellar mass. We derive the bulge mass of each galaxy by multiplying the total stellar mass by a factor f_{bulge}. We assume an average $\langle f_{bulge}\rangle = 0.9$ for all early-type galaxies with $M > 10^{11} M_\odot$ declining to $\langle f_{bulge}\rangle = 0.25$ at $M = 10^{10} M_\odot$, where most red galaxies are in fact lenticular Graham & Worley (2008) and Laurikainen et al. (2010). At each mass, we allow a dispersion of 0.1 around $\langle f_{bulge}\rangle$, i.e. f_{bulge} is drown randomly from the interval $[\langle f_{bulge}\rangle - 0.1, \langle f_{bulge}\rangle + 0.1]$. We assign a random f_{bulge} in the range 0.1–0.3 to late-type (i.e. disc-dominated) galaxies. Although this prescription is somewhat arbitrary, we found that the results are almost independent of f_{bulge} as long as massive early-type galaxies retain a bulge fraction of the order of unity. Given the bulge mass, we estimate L_i by inverting the $M_{bulge}-L_i$ relation given by Sani et al. (2011), and we compute σ by fitting a broken power law to the $z = 0$ $\sigma - M_{bulge}$ data presented by Robertson et al. (2006). This latter conversion implies that a physical MBH population cannot have single-power-law relations with both M_{bulge} and σ, so that our MBH population models are not consistent with each other. As a matter of fact, this has little effect on our computation because the bulk of the signal comes from massive systems ($M_\bullet > 10^8 M_\odot$), for which the $\sigma - M_{bulge}$ is described by a single power law. When converting M_{bulge} into σ, we apply a multiplication factor $(1+z)^{0.3}$, to account for the observational fact that galaxies of a given mass at higher redshift are more concentrated and have larger velocity dispersions than galaxies of the same mass at lower redshift (see e.g. López-Sanjuan et al. 2012). Having derived M_{bulge}, L_i and σ, we can populate galaxies with SMBHs. We apply a further $(1+z)^{0.3}$ correction to the scaling relations involving M_{bulge} and L_i. This redshift dependence improves the match of the SMBH mass density (ρ_{BH}) redshift evolution given by our models with other estimates found the literature (see Fig. 1, lower panel), and we checked that our results are basically independent of it.

Table 2. List of parameters α, β and ϵ. See the text for details. Graham (2012) proposes a double power law with a break at $\bar{M}_{bulge} = 7 \times 10 M_\odot$, values in parentheses refer to $M_{bulge} < \bar{M}_{bulge}$.

Paper	X	α	β	ϵ
Häring & Rix (2004)	M_{bulge}	8.2	1.12	0.30
Sani et al. (2011)	M_{bulge}	8.2	0.79	0.37
Beifiori et al. (2012)	M_{bulge}	7.84	0.91	0.46
McConnell & Ma (2013)	M_{bulge}	8.46	1.05	0.34
Graham (2012)	M_{bulge}	8.56	1.01	0.44
		(8.69)	(1.98)	(0.57)
Sani et al. (2011)	L_i	8.19	0.93	0.38
Gültekin et al. (2009)	σ	8.23	3.96	0.31
Graham et al. (2011)	σ	8.13	5.13	0.32
Beifiori et al. (2012)	σ	7.99	4.42	0.33
McConnell & Ma (2013)	σ	8.33	5.57	0.40
Graham & Scott (2013)	σ	8.28	6.01	0.41

We assign to each merger remnant a total bulge mass equal to the sum of the total stellar masses of the merging systems, i.e. $f_{bulge} = 1$,. Furthermore, we correlate the masses of the merging SMBHs either to the properties of the two merging galaxies or to those of the merger remnant, following the scheme described in section 2.2 of Sesana et al. (2009). This gives us three slightly different mass estimates for the SMBHs forming the binary for each adopted scaling relation.

We combine the $11 \times 3 = 33$ different ways to populate the merging galaxies with SMBHs together with the 216 galaxy merger rates to obtain 7128 different SMBH binary merger rates $d^3n/dz\, dM_{\bullet,1} dq_\bullet$, consistent with current observations of the evolution of the galaxy mass function and pair fractions at $z < 1.3$ and $M > 10^{10} M_\odot$ and with the empirical SMBH–host relations published in the literature. We give equal credit to each model, and we generate 7128 GW signals, sufficient to place reasonable confidence levels for the expected amplitude according to *current observational constraints*. Our approach is modular in nature, and it is straightforward to expand the range of model to include new estimates of all the quantities involved.

2.3 Validation of the models

Although the evolution of the SMBH masses is not followed self-consistently in our models, in Fig. 1 we validate them by comparing the local SMBH mass function and the redshift evolution of the total SMBH density with several estimates found in the literature. We also checked that the predicted range of galaxy and SMBH

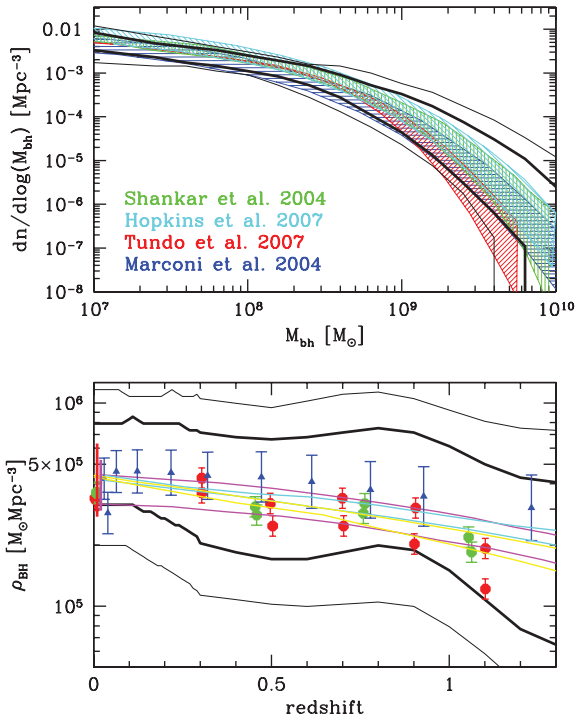

Figure 1. Upper plot: local SMBH mass function. Thick and thin solid black lines enclose the areas corresponding to 68 and 95 per cent confidence levels given by our models. Coloured shaded areas represent SMBH mass functions estimated by Marconi et al. (2004), Shankar et al. (2004), Hopkins, Richards & Hernquist (2007) and Tundo et al. (2007). Lower plot: redshift evolution of the total SMBH mass density. Thick and thin solid black lines have the same meaning as in the upper plot. The red and green dots are from Zhang, Lu & Yu (2012), blue dots are from Hopkins et al. (2007), cyan and yellow lines are from Merloni & Heinz (2008), magenta lines bracket the 1σ uncertainty given by Shankar et al. (2004), the thick magenta and red lines are the estimated uncertainty range at $z = 0$ from Shankar (2009) and Graham & Driver (2007), respectively.

merger rates as a function of mass and redshift are broadly consistent (though with a large scatter) with those derived from our previous models constructed on top of the Millennium Simulation (Sesana et al. 2009) or exploiting semi-analytical merger trees (Sesana et al. 2008). In the latter approach, we evolve the SMBH population self-consistently. In Fig. 1, we show the nominal 1σ and 2σ confidence levels (i.e. the range in which 68 and 95 per cent of our models are contained) of the estimated local SMBH mass function and mass density as a function of z. The agreement with independent results published in the literature is excellent. We notice that we allow for slightly larger values of both quantities with respect to published results. This is because both the McConnell & Ma (2013) and Graham & Scott (2013) scaling relations (that include the recently measured overmassive SMBHs in BCGs) and the double-power-law relation by Graham (2012) predict SMBH masses which are 0.2–0.4 dex larger than previously estimated, particularly at the high-mass end. On the other hand, published SMBH mass functions and mass densities do not include overmassive systems, nor assume a double power law in the SMBH–bulge mass relation.

3 RESULTS AND DISCUSSION

Our main result is shown in Fig. 2, where we plot confidence levels on the GW characteristic amplitude given by our models. When considering the whole set of models (upper-left panel), the 68 per cent

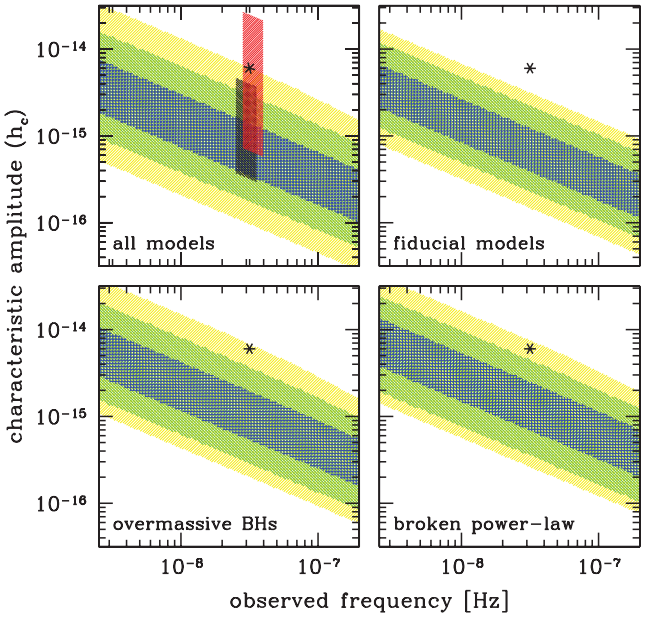

Figure 2. Characteristic amplitude of the GW signal. Shaded areas represent the 68, 95 and 99.7 per cent confidence levels given by our models. In each panel, the black asterisk marks the best current limit from van Haasteren et al. (2011). Shaded areas in the upper-left panel refer to the 95 per cent confidence level given by McWilliams et al. (2012) (red) and the uncertainty range estimated by Sesana et al. (2008). See the text for discussion.

confidence region lies in the range $3.5 \times 10^{-16} < A < 1.5 \times 10^{-15}$, corresponding to a factor of 4 uncertainty in the GW signal. The 99.7 per cent region extends much further, in the range $1.1 \times 10^{-16} < A < 6.3 \times 10^{-15}$, corresponding to a factor of $\approx$50 uncertainty. Note that this latter upper bound is already in tension with the best limit placed by van Haasteren et al. (2011). Our 'democratic' approach to the problem gives the same weight to all the models. One can argue that models featuring the best estimates of the galaxy mass function and pair counts should be considered more robust than those constructed using the upper or lower limits for the same quantities (see Section 2.2.1). If we restrict to 'fiducial models only', the scatter is mildly reduced, and the 68 and 99.7 per cent confidence levels are set in the range $4.0 \times 10^{-16} < A < 1.2 \times 10^{-15}$ and $1.4 \times 10^{-16} < A < 3.1 \times 10^{-15}$, respectively (upper-right panel). If we consider only the SMBH–host relations updated to include the recent measurements of overmassive black hole in BCGs (Graham & Scott 2013; McConnell & Ma 2013), the signal is boosted-up to 68 and 99.7 per cent confidence intervals of $5.6 \times 10^{-16} < A < 2.1 \times 10^{-15}$ and $1.9 \times 10^{-16} < A < 7.1 \times 10^{-15}$, respectively (lower-right panel), a factor of $\approx$2 larger than models featuring previous estimates of the SMBH–host relations. The double-power-law relation of Graham (2012) (lower-left panel) provides similar numbers, even though it does not include overmassive black holes. This is because, compared to linear relations, the 'knee' at $\bar{M}_{\rm bulge}$ implies a higher density of MBHs of a few times $10^8\,{\rm M}_\odot$, which are the ones that contributes the bulk of the signal. Although obtained with a completely different procedure, our confidence intervals are generally consistent with the estimated signal range given by Sesana et al. (2008). The fiducial value provided by McWilliams et al. (2012) is marginally consistent (at a 2σ level in the most favourable scenarios) with our findings. This is not surprising, since their purely merger-driven SMBH evolution naturally produces the highest possible signal for a given SMBH mass function. Within a year, IPTA

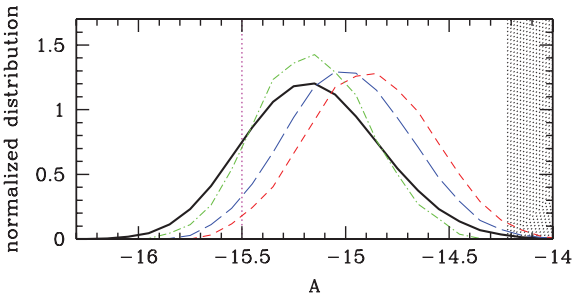

Figure 3. Normalized distributions of the expected GW amplitude A at $f = 1\ \mathrm{yr}^{-1}$. Black solid line, all models; green dot–dashed line, fiducial models only; red short dashed line, models employing the double power law given by Graham (2012); blue long dashed, models including SMBH measurements in BCGs. The shaded area marks the region excluded by current PTA limits, whereas the solid dotted vertical line represents what can be achieved by timing 20 pulsars at 100 ns rms precision for 10 yr.

observations will therefore be able to test their prediction; note however that their 3σ uncertainty range covers one and a half orders of magnitude, with significant overlap to our results. In Fig. 3, we plot the normalized distributions of A given by all our models. The overall distribution (solid black line) has a neat Gaussian shape, in agreement with the central limit theorem. The shaded area, marking the region of A excluded by current limits, already overlaps with the long tails of the distributions. Roughly speaking, the maximum A detectable by a PTA with a signal-to-noise ratio of 5 is roughly given by (Sesana et al. 2008)

$$A \approx 10^{-15} \frac{\delta t_{\rm rms}}{100\,\mathrm{ns}} \left(\frac{N_{\rm p}}{20}\right)^{-1/2} \left(\frac{T_{\rm obs}}{5\,\mathrm{yr}}\right)^{-5/3}, \qquad (6)$$

where $\delta t_{\rm rms}$ is the rms residual of each individual measurement (assumed to be the same for each pulsar), $N_{\rm p}$ is the number of pulsars in the array and $T_{\rm obs}$ is the duration of the experiment. Observations of 20 pulsars at 100 ns rms precision for 10 yr will therefore allow us to detect a signal of $A \approx 3 \times 10^{-16}$ (dotted vertical line in Fig. 3), which encompasses more than 80 per cent of the models presented here.

We should remark at this point that we just considered the expected average signal level, without dealing with any of the issues related to its complicated nature, and to the data processing pipelines. As already mentioned (see also Sesana et al. 2009; Ravi et al. 2012) the signal will likely depart significantly from the smooth stochastic background approximation, which will, in turn, affect its detectability. A lot of work in this direction is undergoing within the IPTA community. Moreover, we considered circular binaries driven by GW only. Even though this is a plausible scenario, other physical mechanisms (stellar scattering, gas torques) can be important for the SMBH binary evolution, impacting also the eccentricity of the systems. We defer the investigation of these issues to future work. Keeping in mind these caveats, our detailed analysis implies that, with an improvement of a factor of only three-to-five on current limits, there is a non negligible chance to make the first ever direct GW detection within the next five years. Even a negative result will nevertheless allow us to constrain the assembly of the most massive galaxies at low-redshift and how do they correlate with their hosts, turning PTAs into useful astrophysical probes.

ACKNOWLEDGEMENTS

AS acknowledges the support of the colleagues in the EPTA and of the DFG grant SFB/TR 7 Gravitational Wave Astronomy and by DLR (Deutsches Zentrum fur Luft- und Raumfahrt), and thanks the referee for valuable suggestions.

REFERENCES

Beifiori A., Courteau S., Corsini E. M., Zhu Y., 2012, MNRAS, 419, 2497
Bell E. F., McIntosh D. H., Katz N., Weinberg M. D., 2003, ApJS, 149, 289
Borch A. et al., 2006, A&A, 453, 869
Bundy K., Fukugita M., Ellis R. S., Targett T. A., Belli S., Kodama T., 2009, ApJ, 697, 1369
de Ravel L. et al., 2009, A&A, 498, 379
Demorest P. B. et al., 2013, ApJ, 762, A94
Drory N. et al., 2009, ApJ, 707, 1595
Ferdman R. D. et al., 2010, Class. Quantum Gravity, 27, 084014
Graham A. W., 2012, ApJ, 746, 113
Graham A. W., Driver S. P., 2007, MNRAS, 380, L15
Graham A. W., Scott N., 2013, ApJ, 764, A151
Graham A. W., Worley C. C., 2008, MNRAS, 388, 1708
Graham A. W., Onken C. A., Athanassoula E., Combes F., 2011, MNRAS, 412, 2211
Gültekin K. et al., 2009, ApJ, 698, 198
Häring N., Rix H.-W., 2004, ApJ, 604, L89
Hlavacek-Larrondo J., Fabian A. C., Edge A. C., Hogan M. T., 2012, MNRAS, 424, 224
Hobbs G. et al., 2010, Class. Quantum Gravity, 27, 084013
Hopkins P. F., Richards G. T., Hernquist L., 2007, ApJ, 654, 731
Ilbert O. et al., 2010, ApJ, 709, 644
Jaffe A. H., Backer D. C., 2003, ApJ, 583, 616
Jenet F. A. et al., 2006, ApJ, 653, 1571
Jenet F. A. et al., 2009, e-prints (arXiv:0909.1058)
Kitzbichler M. G., White S. D. M., 2008, MNRAS, 391, 1489
Laurikainen E., Salo H., Buta R., Knapen J. H., Comerón S., 2010, MNRAS, 405, 1089
López-Sanjuan C. et al., 2012, A&A, 548, A7
Lotz J. M., Jonsson P., Cox T. J., Primack J. R., 2010, MNRAS, 404, 575
Manchester R. N. et al., 2013, Publ. Astron. Soc. Aust., 30, A017
Marconi A., Risaliti G., Gilli R., Hunt L. K., Maiolino R., Salvati M., 2004, MNRAS, 351, 169
McConnell N. J., Ma C.-P., 2013, ApJ, 764, A184
McWilliams S. T., Ostriker J. P., Pretorius F., 2012, e-prints (arXiv:1211.4590)
Merloni A., Heinz S., 2008, MNRAS, 388, 1011
Phinney E. S., 2001, e-prints (arXiv:astro-ph/0108028)
Rajagopal M., Romani R. W., 1995, ApJ, 446, 543
Ravi V., Wyithe J. S. B., Hobbs G., Shannon R. M., Manchester R. N., Yardley D. R. B., Keith M. J., 2012, ApJ, 761, A84
Robertson B., Hernquist L., Cox T. J., Di Matteo T., Hopkins P. F., Martini P., Springel V., 2006, ApJ, 641, 90
Sani E., Marconi A., Hunt L. K., Risaliti G., 2011, MNRAS, 413, 1479
Scott N., Graham A. W., Schombert J., 2013, ApJ, 768, 76
Sesana A., Vecchio A., Colacino C. N., 2008, MNRAS, 390, 192
Sesana A., Vecchio A., Volonteri M., 2009, MNRAS, 394, 2255
Shankar F., 2009, New Astron. Rev., 53, 57
Shankar F., Salucci P., Granato G. L., De Zotti G., Danese L., 2004, MNRAS, 354, 1020
Springel V. et al., 2005, Nat, 435, 629
Tundo E., Bernardi M., Hyde J. B., Sheth R. K., Pizzella A., 2007, ApJ, 663, 53
van den Bosch R. C. E., Gebhardt K., Gültekin K., van de Ven G., van der Wel A., Walsh J. L., 2012, Nat, 491, 729
van Haasteren R. et al., 2011, MNRAS, 414, 3117
Wyithe J. S. B., Loeb A., 2003, ApJ, 590, 691
Xu C. K., Zhao Y., Scoville N., Capak P., Drory N., Gao Y., 2012, ApJ, 747, 85
Zhang X., Lu Y., Yu Q., 2012, ApJ, 761, A5

This paper has been typeset from a TEX/LATEX file prepared by the author.